Supplementary Information (SI) for Analytical Methods.
This journal is © The Royal Society of Chemistry 2025

Novel TICT-characterized fluorescent probes for efficient imaging of lipid droplets in nonalcoholic fatty liver disease

Dongxu Yang,[a†] Tianyi Qu,[b†] Ling Teng,[a] Caihui Wang,[a] Weiyi Bai,[a] Shufen Li,[b*] Weihua Zhuang,[a*] Wengchuang Hu[a*]

[a] Department of Laboratory Medicine/Clinical Laboratory Medicine Research Center, West China Hospital, Sichuan University, Chengdu 610041, Sichuan, China.

[b] Laboratory of Cardiac Structure and Function, Institute of Cardiovascular Diseases, West China Hospital, Sichuan University, Chengdu, 610041, China.

[†] Dongxu Yang and Tianyi Qu contributed equally to this work.

* Corresponding author, Email address: lisf20@scu.edu.cn (S. Li), weihuaz@scu.edu.cn (W. Zhuang) and huwenchuang@wchscu.cn (W. Hu).

Experimental

Figure S20 Merged images of HeLa cells stained with **DAI-LD**.
Figure S21 DAB-LD and **DAI-LD** stained HeLa cells pretreated with starvation (without FBS).
Figure S22 Quantification of LDs number, average LDs size and FL intensity in Figure S21.
Figure S23 H&E, Oil Red O and Masson staining results of liver tissue from a healthy mouse (control) and a mouse with nonalcoholic fatty liver.

Experimental

Materials

4-(N, N-Dimethylamino)phenylborate, 4-bromobenzaldehyde, 1,3-indanedione, cesium fluoride, triethylamine, malononitrile, oleic acid, bis(tri-tert-butylphosphine) palladium (0) ($Pd(t\text{-}Bu_3P)_2$) and 3-(4,5-dimethylthiazol-2-yl)-2,5-diphenyltetrazolium bromide (MTT) were purchased from Adamas Reagent, Ltd. (Shanghai, China). All the other chemicals and solvents were used as received without further purification.

Characterization

NMR spectra were measured on a Bruker AV II-400. Absorption spectra were obtained on a HITACHI U-2910 spectrometer. An Edinburgh FS5 fluorescence spectrometer was used to study the fluorescence emission spectrum. The absolute fluorescence quantum yield of probes was studied via an integrating sphere. A Thermo Scientific Q Exactive (ESI) was used to obtain high-resolution mass spectra (HR-MS). A Leica Stellaris 5 confocal laser scanning microscope (CLSM) was used to image cells stained with probes.

Animal experiments

All animal experiments were approved by the Sichuan Provincial Committee for Experimental Animal Management and performed according to the institutional and NIH guidelines for the care and use of research animals.

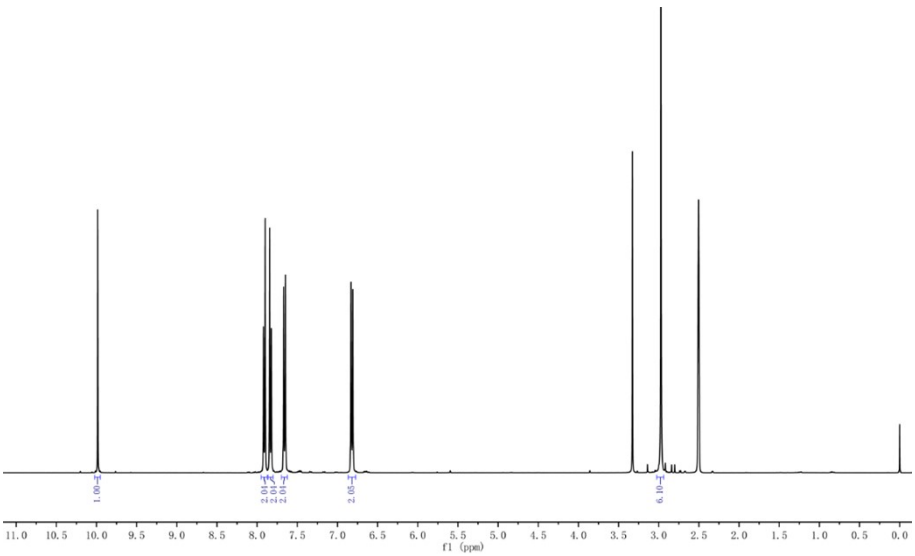

Figure S1 ^{1}H NMR spectrum of compound 1 in DMSO-d_6.

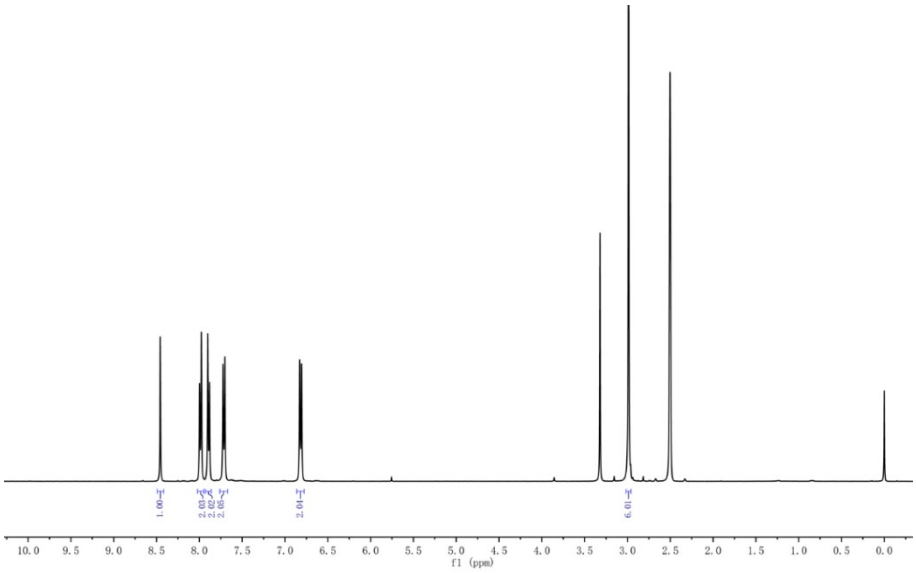

Figure S2 ^{1}H NMR spectrum of **DAB-LD** in DMSO-d_6.

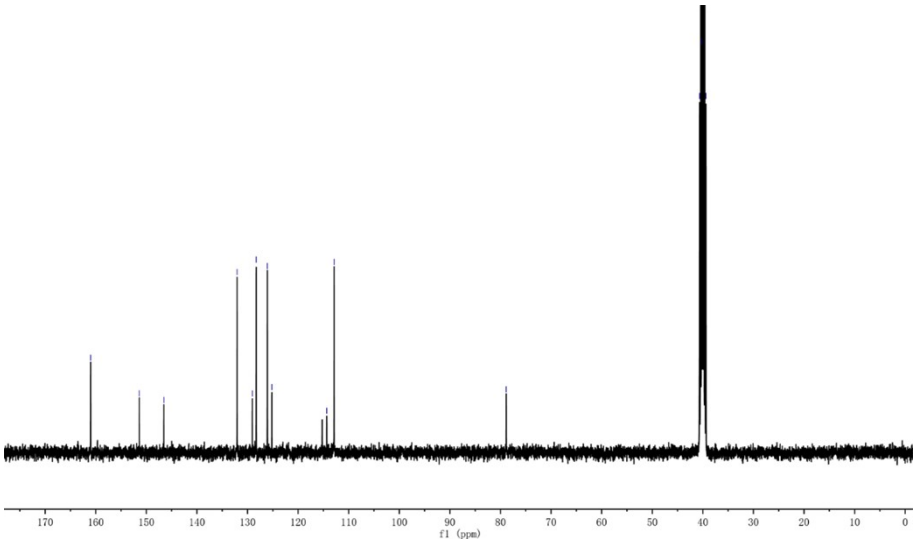

Figure S3 ^{13}C NMR spectrum of **DAB-LD** in DMSO-d_6.

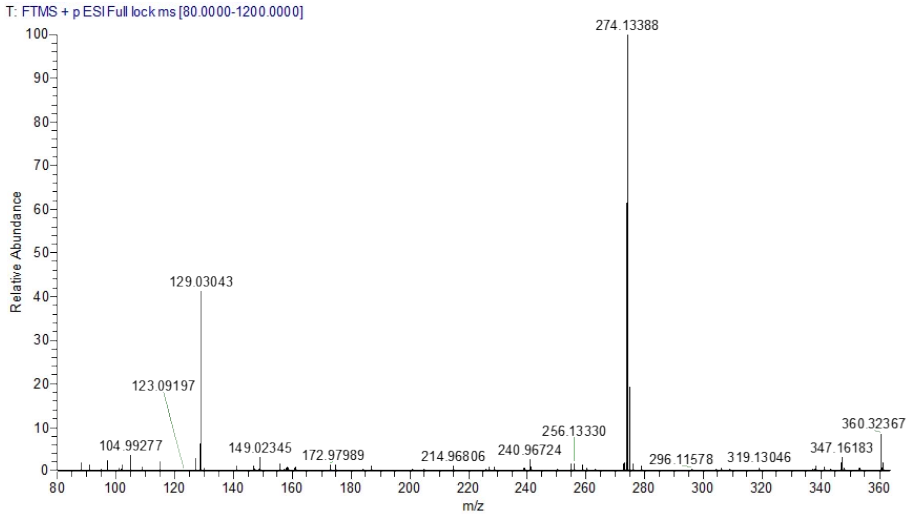

Figure S4 HRMS spectrum of **DAB-LD**.

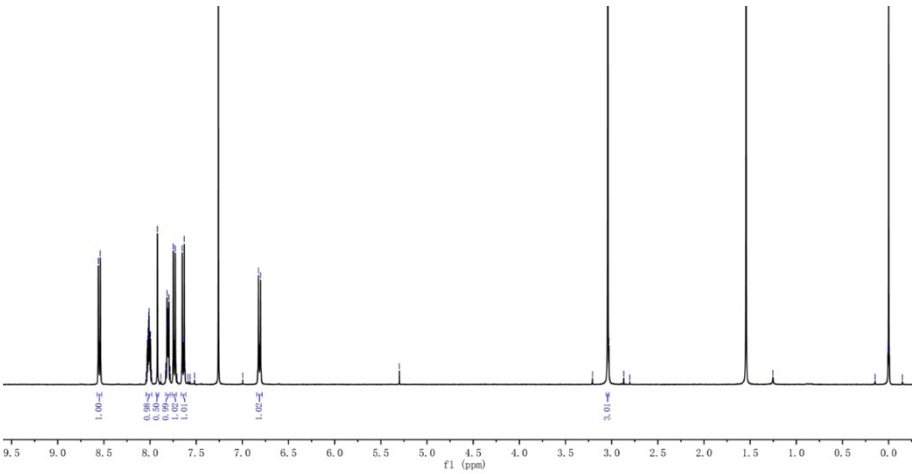

Figure S5 ^{1}H NMR spectrum of **DAI-LD** in $CDCl_3$.

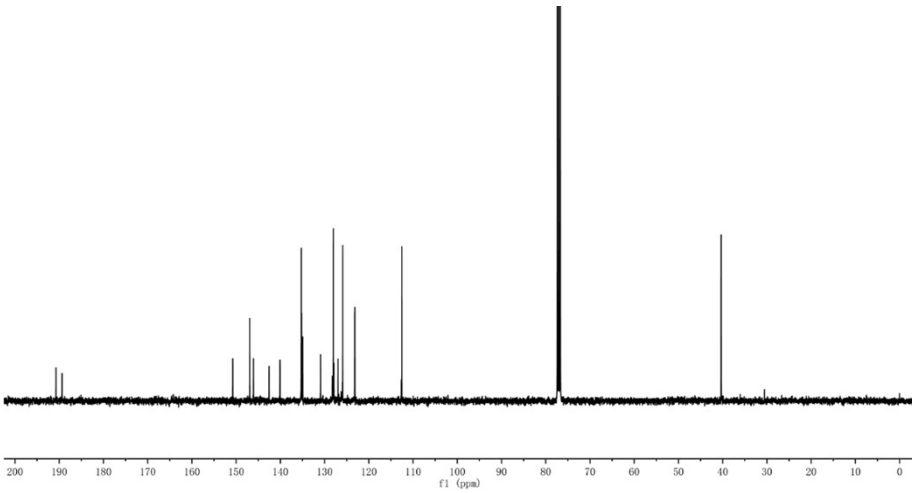

Figure S6 ^{13}C NMR spectrum of **DAI-LD** in $CDCl_3$.

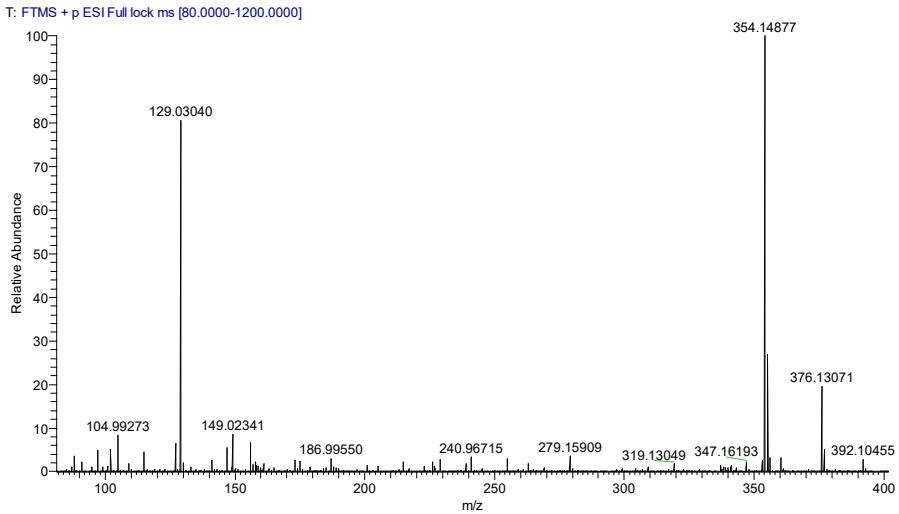

Figure S7 HRMS spectrum of **DAI-LD**.

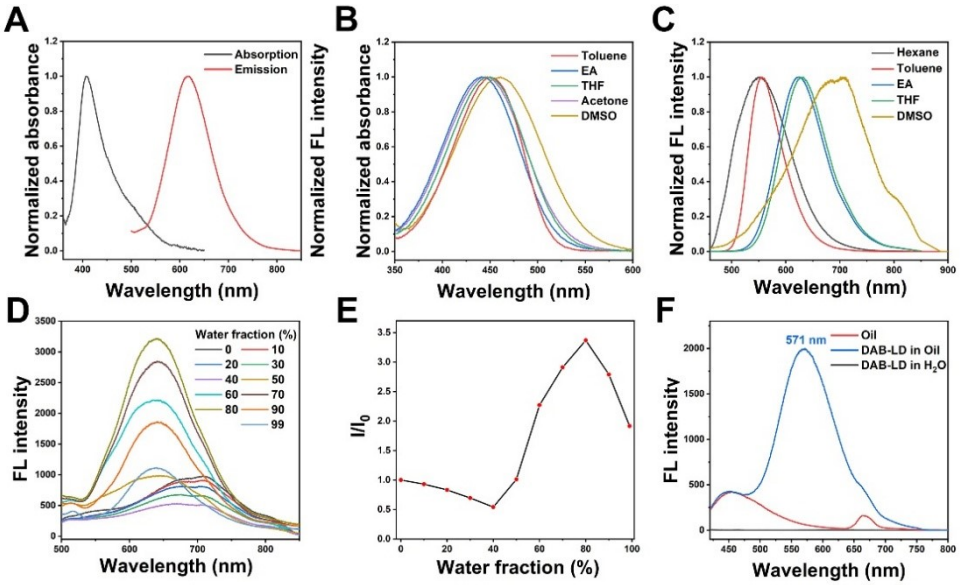

Figure S8 Photophysical studies of **DAB-LD**. Normalized absorption and FL spectra of **DAB-LD** in H_2O (A). Normalized absorption spectra of **DAB-LD** in different solvents (B). Normalized FL spectra of **DAB-LD** in different solvents (C). FL spectra of **DAB-LD** in mixtures of DMSO and H_2O with different H_2O fractions (D). Changes of fluorescent intensity of **DAB-LD** in DMSO/water mixtures with different water fractions (E). FL spectra of **DAB-LD** in oil and H_2O (F). λ_{ex} = 408 nm.

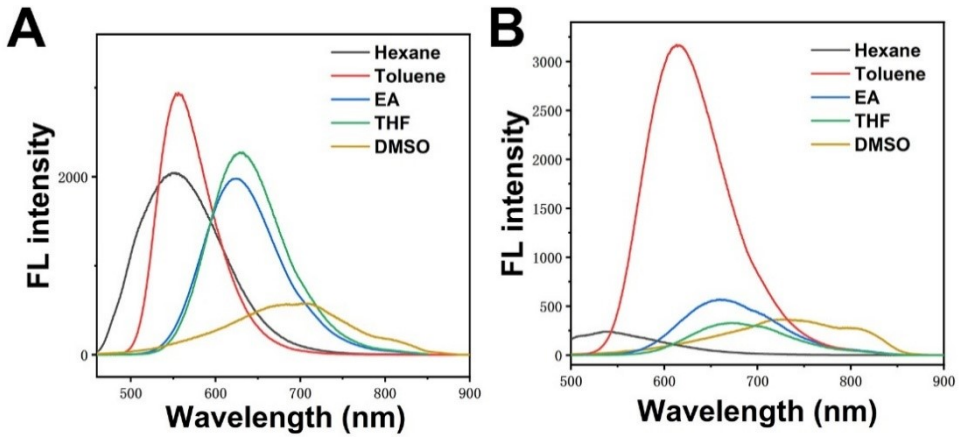

Figure S9 FL spectra of **DAB-LD** in different solvents (A). FL spectra of **DAI-LD** in different solvents (B).

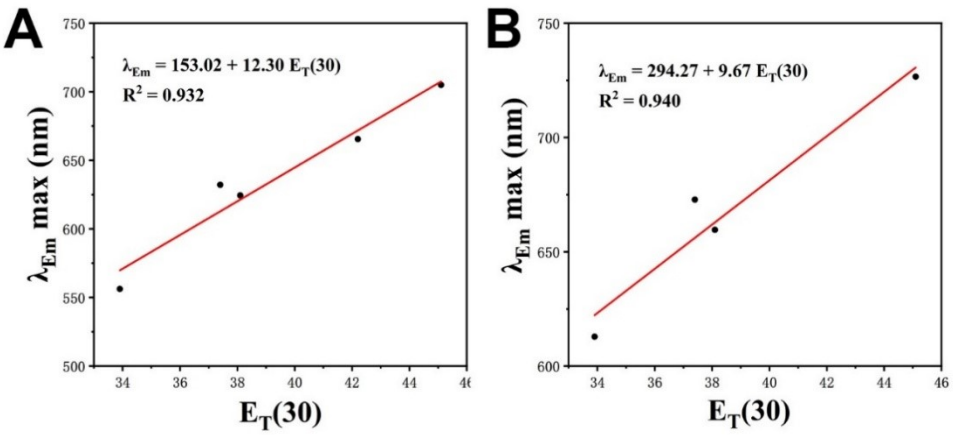

Figure S10 Linear relationship between the maximum emission wavelength and the solvent's polarity of **DAB-LD** (A). Linear relationship between the maximum emission wavelength and the solvent's polarity of **DAI-LD** (B).

Table S1 Fluorescence quantum yield (Φ) of probes in different solvents

Probe	Solvent	Fluorescence quantum yield (Φ) (%)
DAB-LD	DMSO/H_2O = 99/1	~0
	DMSO/H_2O = 1/99	~0
	toluene	37.78
	oleic acid	85.20
DAI-LD	DMSO/H_2O = 99/1	~0
	DMSO/H_2O = 1/99	~0
	toluene	33.39
	oleic acid	22.76

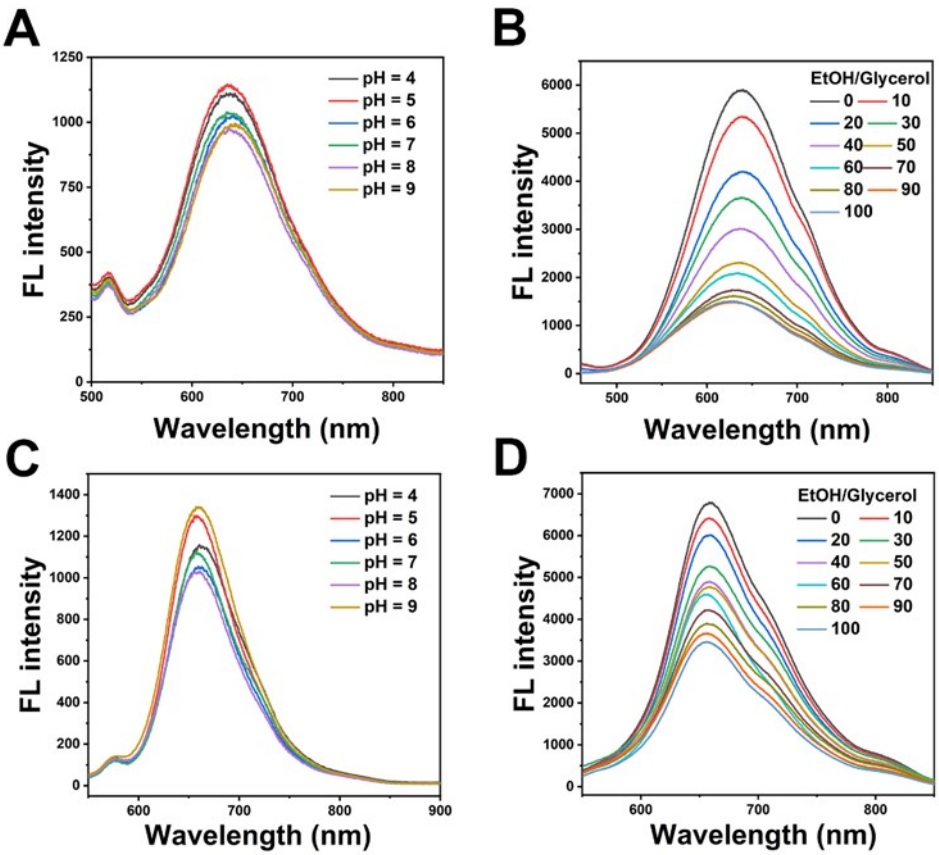

Figure S11 FL spectra of **DAB-LD** with different pH (A). FL spectra of **DAB-LD** in EtOH/glycerol mixed solution (B). FL spectra of **DAI-LD** with different pH (C). FL spectra of **DAI-LD** in EtOH/glycerol mixed solution (D).

Table S2. A comparison of some reported fluorescent probes with **DAB-LD** and **DAI-LD**.

Probe	$\lambda_{abs}/\lambda_{em}$ (nm)	Stokes shift	Φ^a	Φ^b	Lowest staining concentration	Ref.
DAB-LD	408/615 (water)	207 nm	0.852	~0	0.5 μM	This work
DAI-LD	435/707 (water)	272 nm	0.2276	~0	0.5 μM	This work
Flp-12	467/567 (water)	100 nm	—	4.42×10^{-3}	0.5 μM	(1)
LD-TTP	416/548 (water)	132 nm	—	3.3×10^{-3}	3 μM	(2)
ANI	523/627 (DMSO)	104 nm	0.126	5.1×10^{-3}	1 μM	(3)
lip-YB	512/693 (water)	181 nm	0.7328	1.03×10^{-2}	3 μM	(4)
CCB	503/659 (DMSO)	156 nm	—	5×10^{-2}	10 μM	(5)

B2	421/507 (DMSO)	86 nm	—	7×10^{-4}	10 μM	(6)
TPABSM	460/605 (Toluene)	145 nm	—	—	2 μM	(7)
LD1	499/639 (DMSO)	140 nm	—	7×10^{-3}	1 μM	(8)

[a]Fluorescence quantum yield in oleic acid. [b]Fluorescence quantum yield in H_2O or DMSO.

(1) G. Jiang, Y. Jin, M. Li, H. Wang, M. Xiong, W. Zeng, H. Yuan, C. Liu, Z. Ren and C. Liu, Anal Chem, **2020**, 92, 10342-10349.

(2) L. Fan, X. Wang, Q. Zan, L. Fan, F. Li, Y. Yang, C. Zhang, S. Shuang and C. Dong, Analytical Chemistry, **2021**, 93, 8019-8026.

(3) C.-J. Wu, X.-Y. Li, T. Zhu, M. Zhao, Z. Song, S. Li, G.-G. Shan and G. Niu, Analytical Chemistry, **2022**, 94, 3881-3887.

(4) H. Huang, Y. Bu, Z.-P. Yu, M. Rong, R. Li, Z. Wang, J. Zhang, X. Zhu, L. Wang and H. Zhou, Analytical Chemistry, **2022**, 94, 13396-13403.

(5) C. Lai, Y. Zhao, X. Zou, Y. Liang and W. Lin, Sensors and Actuators B: Chemical, **2022**, 369, 132267.

(6) H. Wang, C. Zhang, X. Shen, Z. Wang, J. Yang, S. Shen, L. Hu, J. Pan and X. Gu, Dyes and Pigments, **2023**, 212, 111137.

(7) Y. Yu, H. Xing, H. Park, R. Zhang, C. Peng, H. H. Y. Sung, I. D. Williams, C. Ma, K. S. Wong, S. Li, Q. Xiong, M.-H. Li, Z. Zhao and B. Z. Tang, ACS Materials Letters, 2022, 4, 159-164.

(8) H. W. Lee, I.-J. Lee, S.-J. Lee, Y. R. Kim and H. M. Kim, ACS Sensors, 2022, 7, 1027-1035.

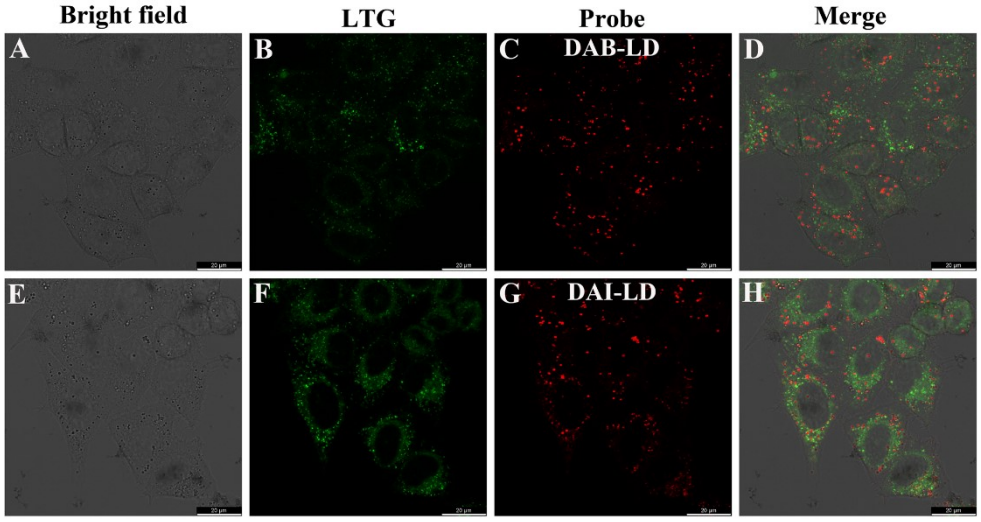

Figure S12 Colocalization study of the probes with LysoTrack Green (LTG). Bright field of HeLa cells stained with (A) **DAB-LD** and (E) **DAI-LD**. Confocal images of HeLa cells stained with **DAB-LD** (C, λ_{ex} = 488 nm, λ_{em} = 600–650 nm), **DAI-LD** (G, λ_{ex} = 488 nm, λ_{em} = 600–650 nm) and LTG (100 nM, λ_{ex} = 488 nm, λ_{em} = 510–550 nm) (B and F). (D) Merged image of (A), (B) and (C). (H) merged image of (E), (F) and (G). Scale bar = 20 μm.

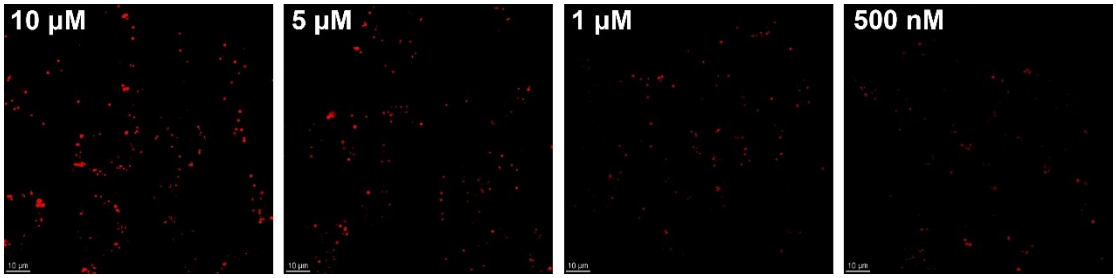

Figure S13 CLSM images of HeLa cells stained with different concentrations of **DAB-LD** (λ_{ex} = 488 nm, λ_{em} = 550–650 nm). Scale bar = 10 μm.

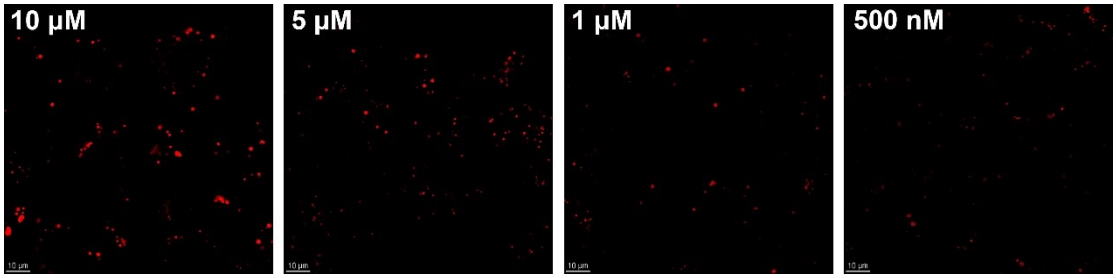

Figure S14 CLSM images of HeLa cells stained with different concentrations of **DAI-LD** (λ_{ex} = 488 nm, λ_{em} = 550–650 nm). Scale bar = 10 μm.

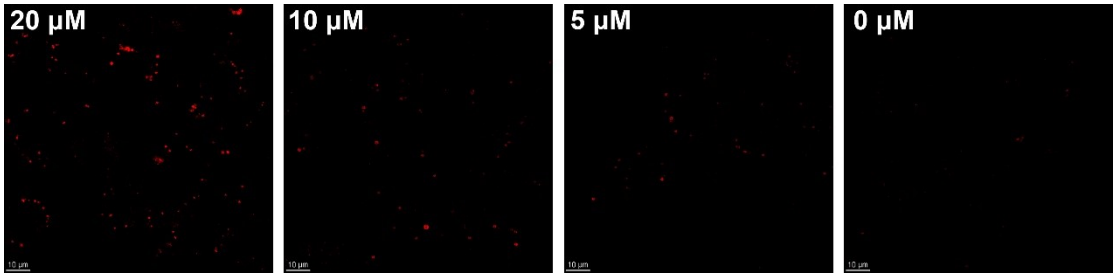

Figure S15 CLSM images of HeLa cells untreated or pretreated with different concentrations of oleic acid stained by **DAB-LD**. Scale bar = 10 μm.

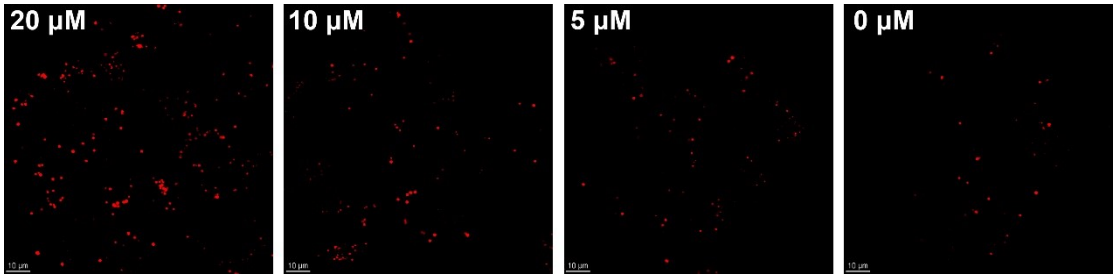

Figure S16 CLSM images of HeLa cells untreated or pretreated with different concentrations of oleic acid stained by **DAI-LD**. Scale bar = 10 μm.

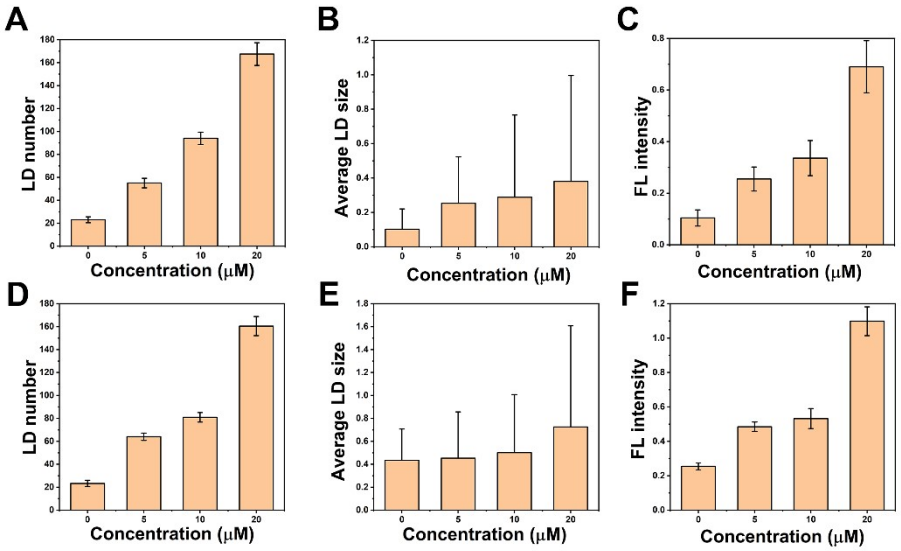

Figure S17 Quantification of LDs number in Figure S15 (A) and Figure S16 (D). Quantification of average LDs size in Figure S15 (B) and Figure S16 (E). Quantification of FL intensity in Figure S15 (C) and Figure S16 (F).

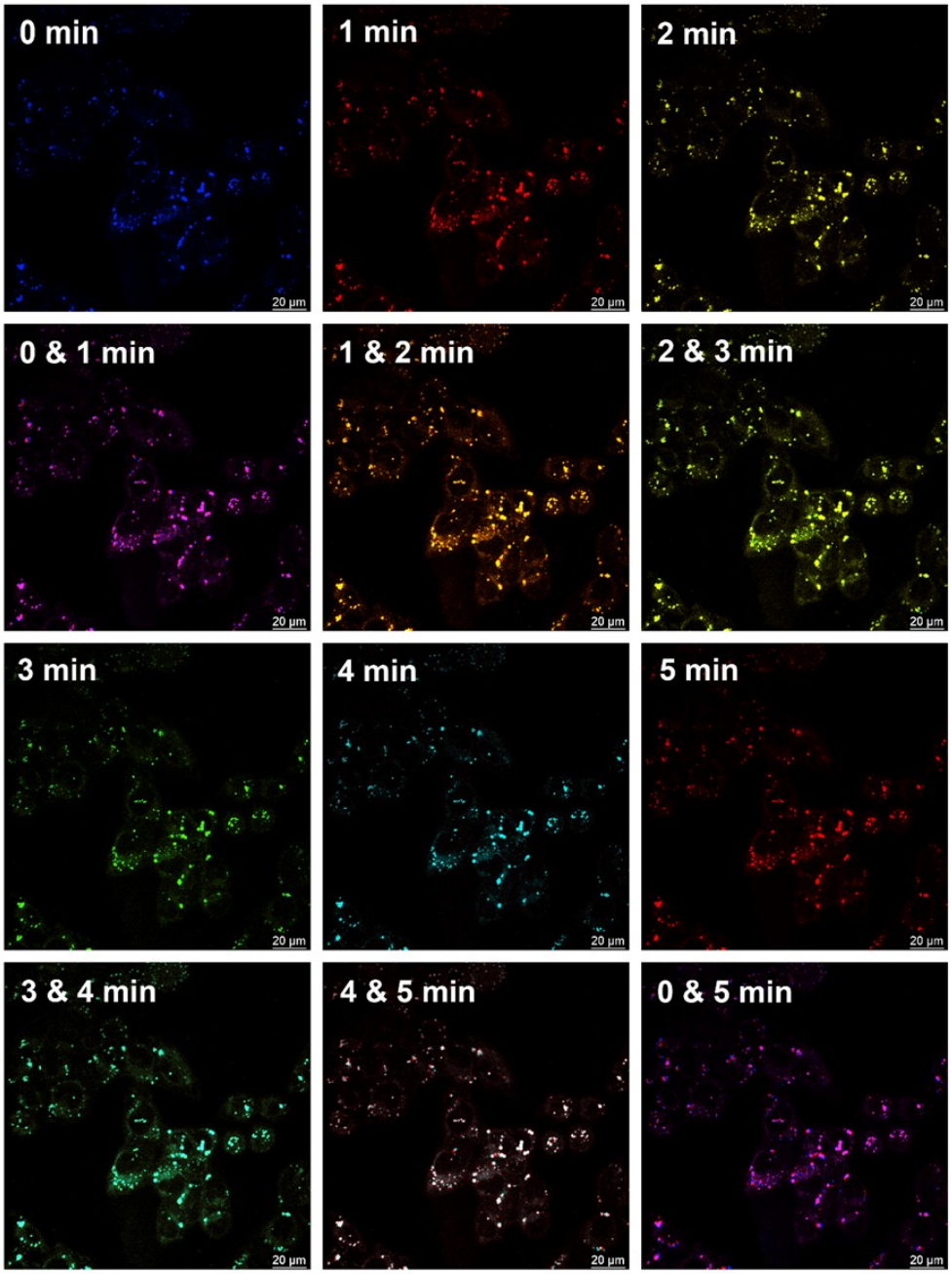

Figure S18 Temporal scanning images of HeLa cells stained with **DAB-LD** (λ_{ex} = 488 nm, λ_{em} = 550–650 nm). Time = 5 min. Scale bar = 20 μm.

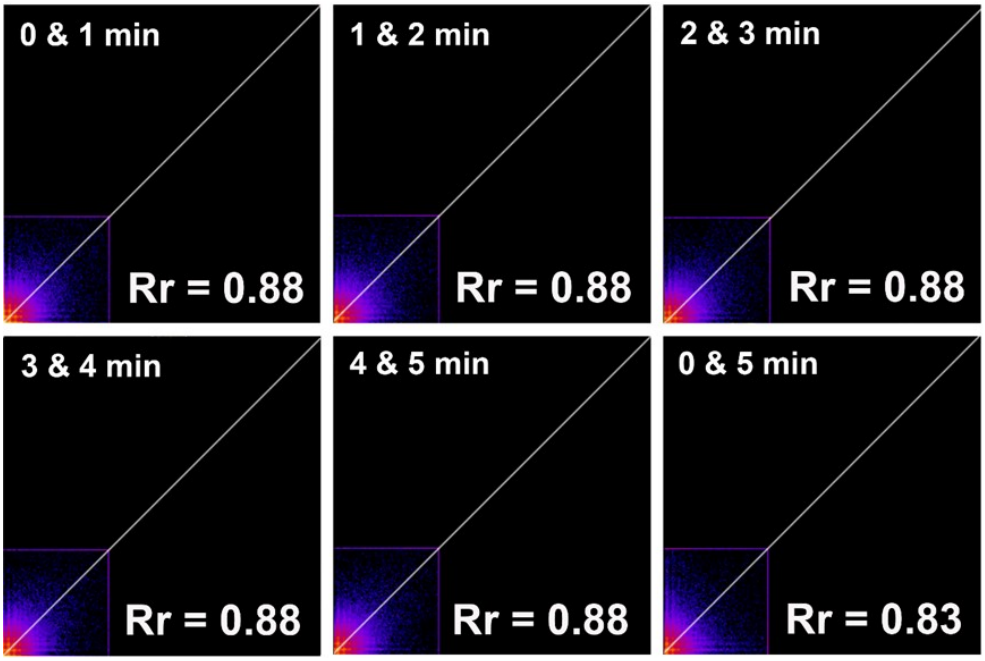

Figure S19 Merged images of HeLa cells stained with **DAB-LD** in Figure S18.

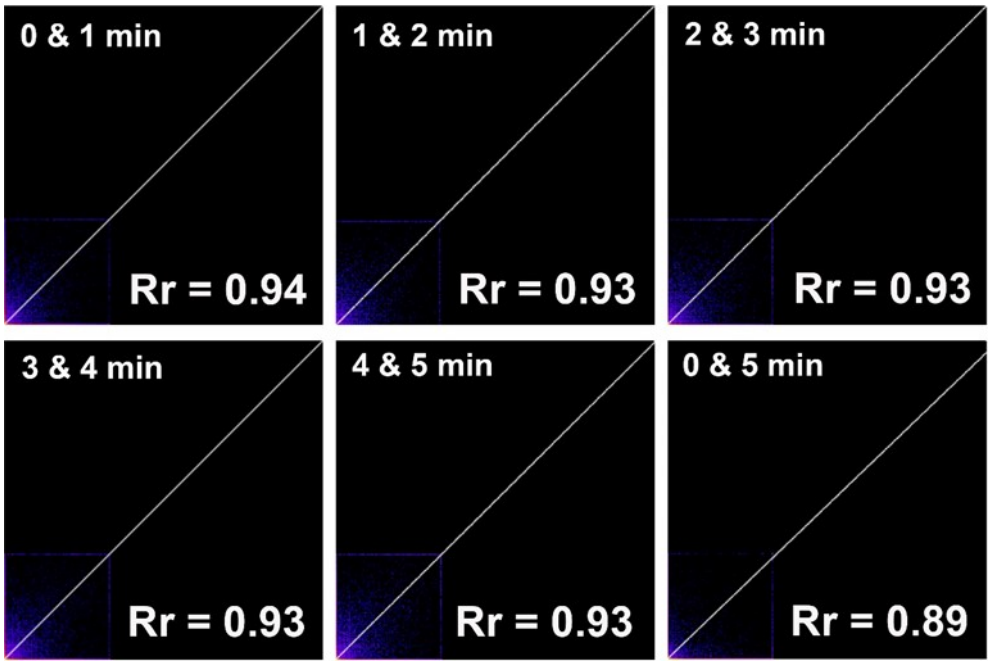

Figure S20 Merged images of HeLa cells stained with **DAI-LD** in Figure 5.

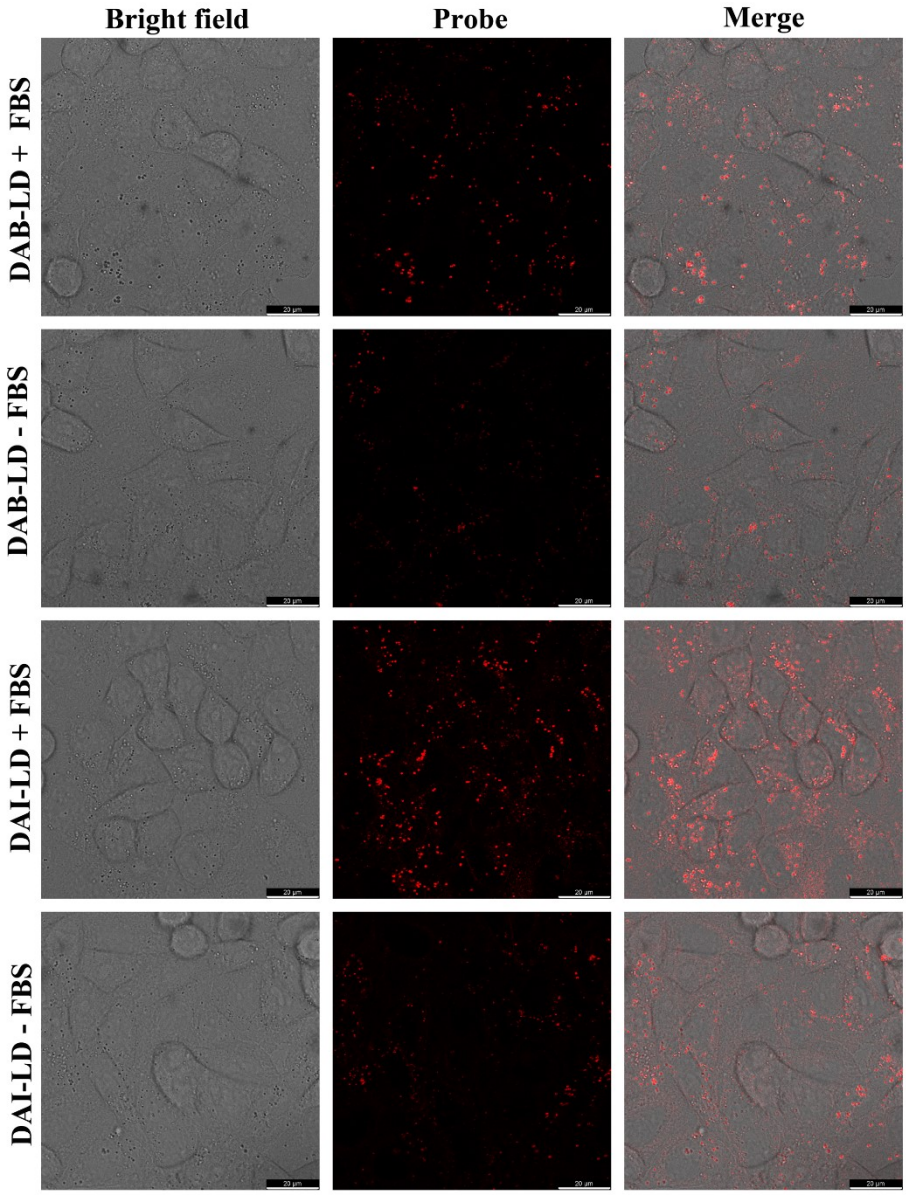

Figure S21 DAB-LD and **DAI-LD** stained HeLa cells pretreated with starvation (without FBS). +FBS indicating the control group with 10% FBS, -FBS indicating the experimental group pretreated with starvation.

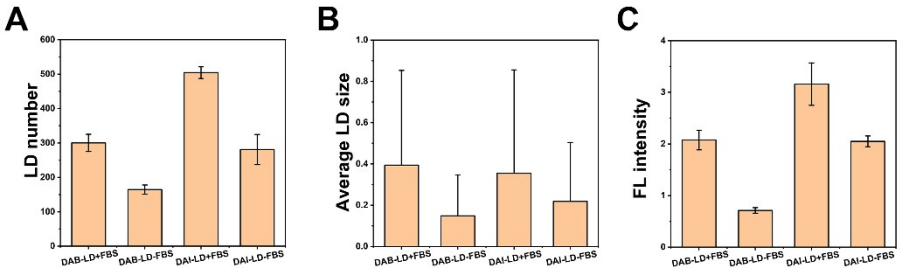

Figure S22. Quantification of LDs number in Figure S21 (A). Quantification of average LDs size in Figure S21 (B). Quantification of FL intensity in Figure S21 (C).

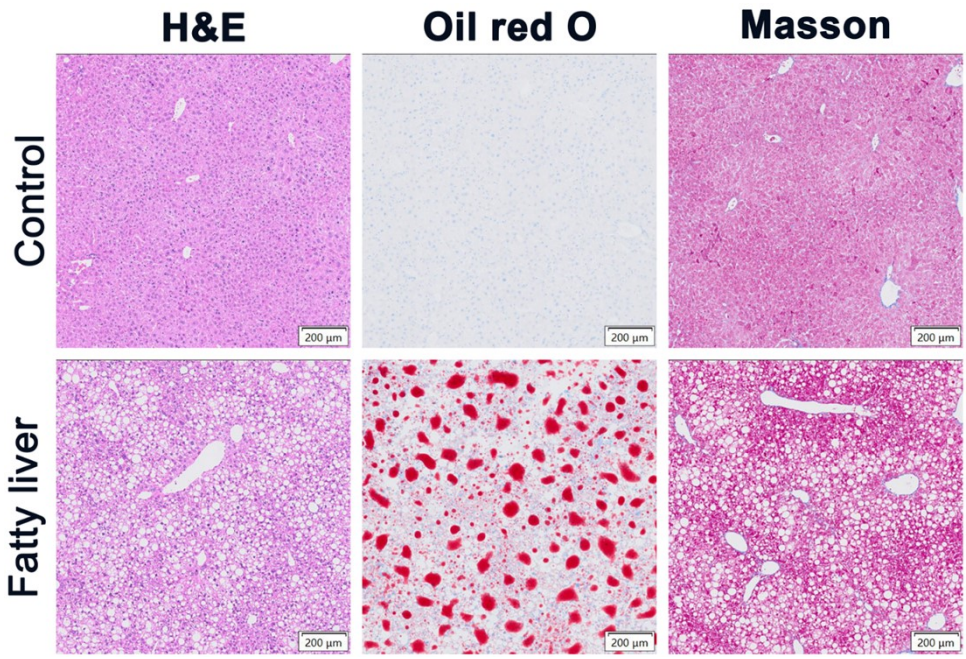

Figure S23 H&E, Oil Red O and Masson staining results of liver tissue from a healthy mouse (control) and a mouse with nonalcoholic fatty liver.